



Energy Saving of Heat Gain by Using Buried Pipe Inside a Roof

Ahmed A. M. Saleh

Department of Mechanical Engineering / University of Technology

E-mail: aamsaleh60@yahoo.com

(Received 6 July 2014; accepted 28 December 2014)

Abstract

This work deals with a numerical investigation to evaluate the utilization of a water pipe buried inside a roof to reduce the heat gain and minimize the transmission of heat energy inside the conditioning space in summer season. The numerical results of this paper showed that the reduction in heat gain and energy saving could be occurred with specific values of parameters, like the number of pipes per square meter, the ratio of pipe diameter to the roof thickness, and the pipe inlet water temperature. Comparing with a normal roof (without pipes), the results indicated a significant reduction in energy heat gain which is about 37.8% when the number of pipes per meter of roof length is 3.0, the ratio of pipe diameter to the wall thickness (D/W) is 0.20, and the water inlet temperature is 30°C, while the minimum ratio of reduction 24% is achieved when the number of pipes per meter, the ratio of pipe diameter to the wall thickness, and the water inlet temperature are 27, 30 and 33 °C, respectively. The results also showed that there is a very small effect of pipe centre position inside the wall on the final heat transmission.

Keyword: *Water pipe, Roof heat gain, Solar-air temperature.*

1. Introduction

The energy performance of a building has become an important factor in the design of the building. It was found that approximately 49% of the site's electricity consumption has been used in the HVAC system, as shown in Fig. 1., therefore the deep studying of cooling load component is essentially important especially in the hot areas. Lee (1993) used a computer simulation to analyse the energy performance of the various energy conservation measures with respect to the design of commercial buildings. The design referred to the building shape, size, texture, lighting level, etc. The results showed that there was a possibility of 40% energy reduction from a combination of design improvements. Thus, it is important to include the energy efficiency as a criteria during the design stage. Hoo (2001) focused on the energy usage in air-conditioning system. His thesis had covered the various types of air-conditioning system in the markets and ways to conserve energy. It also touched on the benefits of using BAS (Building Automation

system) in conserving energy use in air-conditioning system.

Tawee Vechaphitt [2] studied the effect of variation of shape and orientation of a building on the average heat gain, and analyzed the optimum shape of the building to minimize the average heat gain. In order to provide guidelines for reduction of that gain through the buildings, comparisons were made using four thermal insulating materials.

Sebashtain [3] treated the modelling and testing of hollow core concrete elements for heat storage and eat distribution via building construction thermally activated building system, using ventilated hollow core concrete element. This system is analysed as well as optimized for effective use of low valued energy sources. This leads to confirm the biggest advantage of system is the capability to store and distribute heat in the hollow core concrete which has a positive effect on energy use.

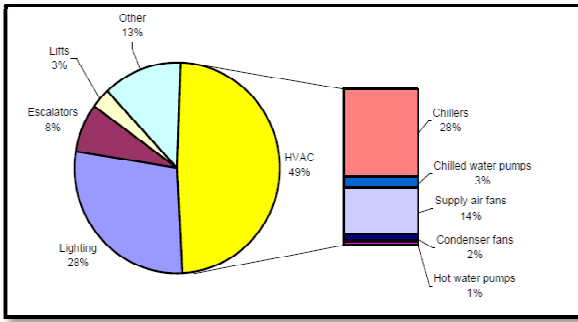


Fig. 1. Electricity power consumption [1].

R. Saidur and others [4] studied the overall thermal transfer value (OTTV) and the energy consumption of room air conditioning of the residential building (Malaysia). It was found that OTTV of the residential building varies from 35 to 65 W/m² with a mean value of 41.7 W/m². The sensitivities of several parameters, such as window to wall ratio, shading coefficient (SC), U-value for wall and absorption (α) provide the optimum design

T. Kiatsiriroal and M. Veekel [5] find that heat accumulated in the wall of an air conditional building could be excreted by the circulation of water in a set of copper tube embedded at the outer wall surface. They found that the period of cooled wall operation, between 10 am. - 5 pm., the cooling load could be 3.67 kWh/day compared with 4.56 kWh/day, for the normal wall.

Corgnti and Kindinis [6] report a dynamic simulation of an active Hollow core slab using Simulink. The heat transfer in the solid part of the slab in transient conditions is expressed in its typical differential formulation, and is solved with explicit method. The researcher investigated the possibility of using the active hollow core slab to utilize free cooling at night to reduce the energy demand for climate control in Mediterranean countries. Compering a traditional ventilation system with the night ventilation operation, the hollow core ventilation system offered that the application of hollow core slab for utilization the cooling night air can drastically help on reducing summer cooling loads.

Sormunt et al. [7] use advance modelling and simulation analysis and laboratory measurements to develop several concept to integrate thermal mass of hollow core slab air conditioning system. The authors observed by active use of thermal mass showed 4-10 % saving in heating energy, 46-47 % saving in cooling energy and 12-23 % saving in fan energy when compared with traditional system.

2. Theory and Model

In general, the thermal resistance-capacity formulation for the energy balance on a node using backward-difference, shown in Fig. 2., is [8].

$$q_i + \sum \frac{T_j^P - T_i^P}{R_{ij}} = C_i \frac{T_i^{P+1} - T_i^P}{\Delta\tau} \quad \dots (1)$$

Thermal capacity C_i is defined as:

$$C_i = \rho c_p \Delta V_i$$

The solution of equation (1) can be carried out by a number of methods. If the solution is to be performed with Gauss-seidel iteration technique, then equation (1) should be solved for T_i^{P+1} and expressed as:

$$T_i^{P+1} = \left(q_i + \sum_j \frac{T_j^P}{R_{ij}} \right) \frac{\Delta\tau}{C_i} + \left(1 - \frac{\Delta\tau}{C_i} \sum_j \frac{1}{R_{ij}} \right) T_i^P \quad \dots (2)$$

To insure stability, one must keep $\Delta\tau$ equal to or less than the value obtained from the most restrictive nodal by solving for $\Delta\tau$

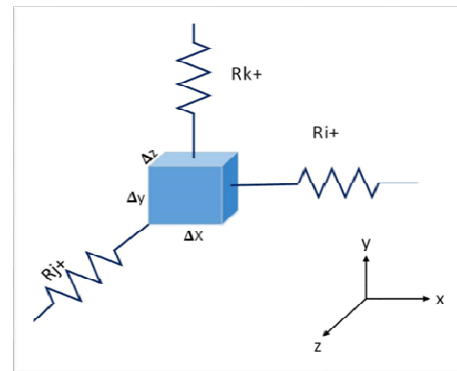


Fig. 2. Element of model.

$$\Delta\tau \leq \left(\frac{C_i}{\sum_j 1/R_{ij}} \right)_{min} \quad \dots (3)$$

The resistance element (R_{ij}), shown in Figure (2), for each node in the roof is given in Table (1).

Table 1,
The resistance of nodes (R_{ij}) [8].

Node condition	R_i^+	R_i^-	R_j^+	R_j^-	R_k^+	R_k^-
Inside the roof	$\frac{K A_x}{\Delta x}$	$\frac{K A_x}{\Delta x}$	$\frac{K A_y}{\Delta y}$	$\frac{K A_y}{\Delta y}$	$\frac{K A_z}{\Delta z}$	$\frac{K A_z}{\Delta z}$
Convection on the outside (h_o)	$\frac{K A_x}{\Delta x}$	$h_o A_x$	$\frac{K A_y}{2\Delta y}$	$\frac{K A_y}{2\Delta y}$	$\frac{K A_z}{2\Delta z}$	$\frac{K A_z}{2\Delta z}$
Convection in the inside (h_i)	$h_i A_x$	$\frac{K A_x}{\Delta x}$	$\frac{K A_y}{2\Delta y}$	$\frac{K A_y}{2\Delta y}$	$\frac{K A_z}{2\Delta z}$	$\frac{K A_z}{2\Delta z}$

2.1. Solar-Air Temperature

Solar air temperature used to estimate the outdoor temperature which is included the effect of local and instantaneous solar radiation, using equitation [9].

$$T_{sat} = T_o + \alpha \frac{G_t}{h_o} - \frac{\epsilon \Delta R}{h_o} \quad \dots (4)$$

2.2. Heat Gain within the Water Pipe

Heat gain from the pipe embedded inside the roof, shown in Fig. 3. , can be estimated by using the energy balance between the nodes:

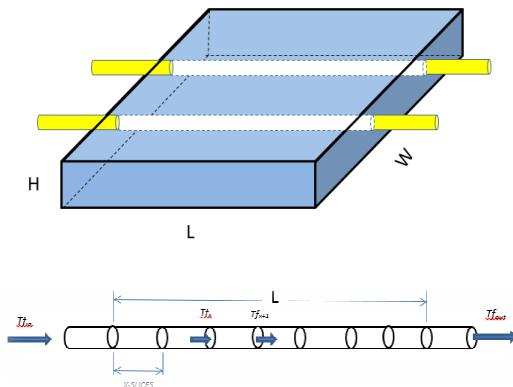


Fig. 3. Water pipe embedded inside the roof.

$$\sum Q_k = \dot{m} c_p \Delta T \quad \dots (5)$$

$$\sum Q_k = \dot{m}_f c_p (T_{f_{k+1}} - T_{f_k}) \quad \dots (6)$$

Solving for $T_{f_{k+1}}$

$$T_{f_{k+1}} = \frac{\sum Q_k}{\dot{m} c_p} + T_{f_k}$$

$$Q_k = h_f A_x \Delta T$$

$$Q_k = h_f A_x (T_{pipe} - T_{f_{ave}}) \quad \dots (7)$$

To find the inside pipe heat transfer coefficient (h_f) using Dittus-Boelter equation for turbulent flow [6],

$$Nu = 0.023 Re^{0.8} Pr^{0.4} \quad \dots (8)$$

$$Nu = \frac{hD}{k} \quad \dots (9)$$

3. Initial and Boundary condition

The initial condition of all nodes in the solution domain is assumed to be the average temperature between the outside and the inside temperature although the value of initial condition is not affecting significantly on the final results. And, the boundary conditions which are employed in the present case study are listed in Table 2.

Table 2,
Boundary conditions.

Value of x, y, and z	Condition	Temp.	Remark
$x=0$	Outside surface	Two	
$x=L$	Inside surface	Two	
$y=0$	Starting of simulation in y-direction	$\frac{\partial T_y}{\partial z}=0$	Similarity y
$y=W$	End length of simulation in y- direction	$\frac{\partial T_y}{\partial z}=0$	Similarity y
$z=0$	Starting of simulation in z-direction	$\frac{\partial T_z}{\partial y}=0$	Similarity y
$z=H$	End length of simulation in z- direction	$\frac{\partial T_z}{\partial y}=0$	Similarity y

4. Program and Solution Code

FORTRAN code was designed to accomplish the numerical solution of the final set of liner equations by Guiss-sedil iterative method (simple and well known) with suitable value of over relaxation factor and a relative error of 1.0×10^{-3} . A grid mesh of a 3-D model is within $70 \times 70 \times 20$. Fig. 4. illustrates the flow chart of the solution scheme.

5. Result and Discussion

Figure (5) represents the temperature distribution contour lines of the concrete roof section (without pipe) at the noon (mid-day), to be compared with other cases. It is clear that the major effect of water pipe on the shape of temperature contour line damped the propagation of high temperature regime to reach the inside surface of the roof, therefore the average temperature of the inside surface will be less and the heat gain entering the space also reduced. That is due to absorbing an important part of a heat transfer inside the space in the wall by flowing water inside buried pipe and pick it away. Figures (6) and (7) show the same effect of pipe on the contour lines but with different size of pipe per thickness of roof ($D/H=0.2$ & 0.4) and also the number of pipes in one meter of roof width is 2.0 in Figure (8).

Figure (9) depicts, the three mode of heat transfer distribution along one day in the normal roof (without pipe). The energy entering the space via the roof (Q_{space}) reached the maximum value at 5 pm with a time lag about 5 hours to transfer of the heat entering the roof from outside (Q_{roof}) due to the heat storage in the room. The minimum heat gain occurred at 8 a.m., because the roof lost most of its storage energy to the outdoor air during the night.

Figure (10) shows the effect of water inlet temperature to the pipe on the heat gain per square meter of roof area. The heat gain reduced about 15-22 % compared with the normal roof on the peak time period, this result support the suggested modification that the use of water inside the concrete roof is feasible and economical.

Figure (11) and Figure (12) explore the low significant effect of pipe position inside the roof and the pipe diameter per roof thickness on the heat transmitted inside the space respectively, the reason of this results could be related to consideration of the analysis on energy through long period (one day) which decays the effect of that parameters

The enhancement in heat gain reduction with increasing the number of pipes per meter of roof span width is more obvious in Figure (13), because the buried pipe works like a heat sink inside the roof.

The effect of the water velocity (Reynolds number) inside the pipe on the heat gain through the roof is shown in Figures (14). Because of increasing the heat transfer coefficient due to high Reynolds number, the heat gain reduction increases.

Figure (15) summarizes the cases that have been studied and mentioned in Table-3, the y axis of the figure represents the accumulating energy entering the space per meter square of roof area per day. Directly, it can be detected that case 7 is the optimum case among the others.

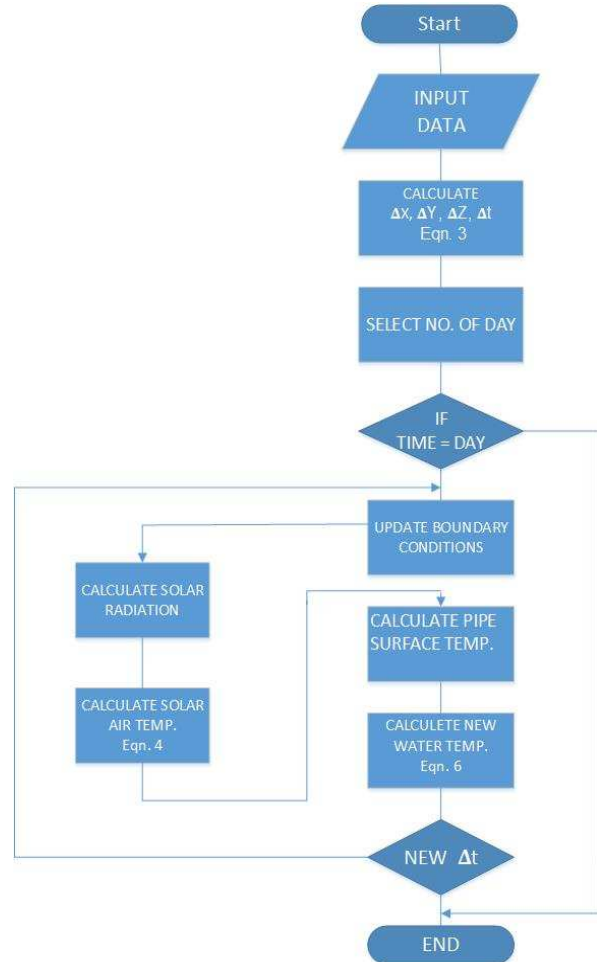


Fig. 4. Program flow chart.

6. Conclusion

The present work reveals the significant effect of buried pipe inside the roof is save the energy consumption in two points. First the reduction of heat gain and then the cooling load of particular space, second the ability of utilize the heat energy cared up from the roof in other useful applications.

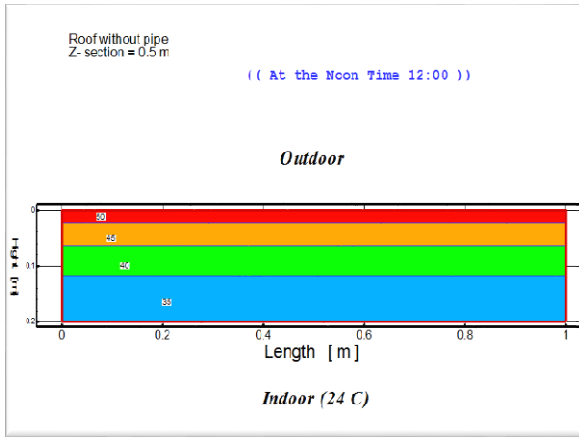


Fig. 5. Contour lines of temperature distribution of Roof without Pipe.

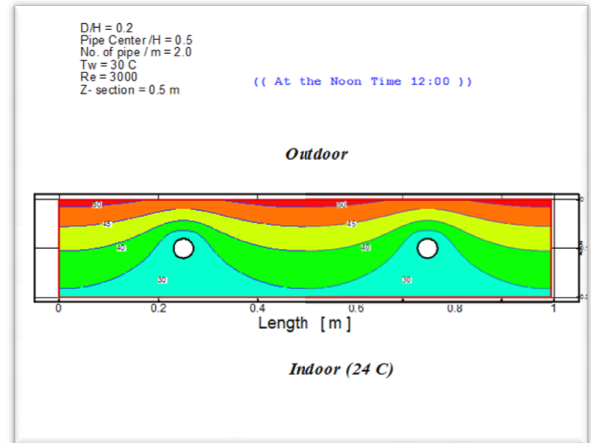


Fig. 8. Contour lines of temperature distribution when $D/H=0.2$, $T_w=30\text{ }^\circ\text{C}$, $Re=3000$, No. of pipe/m=2.

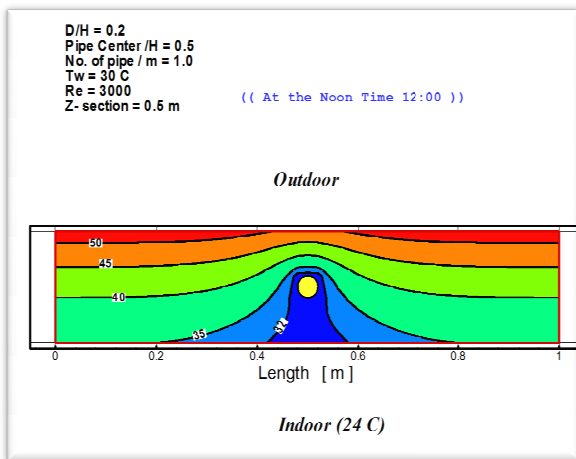


Fig. 6. Contour lines of temperature distribution when $D/H=0.2$, $T_w=30\text{ }^\circ\text{C}$, $Re=3000$.

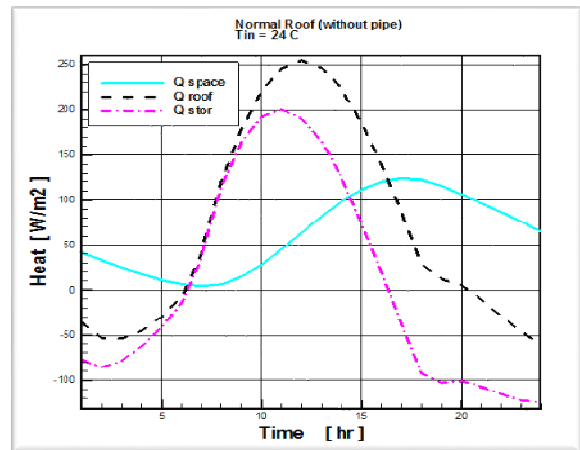


Fig. 9. Heat gain distribution in the roof versus time for normal roof (without pipes).

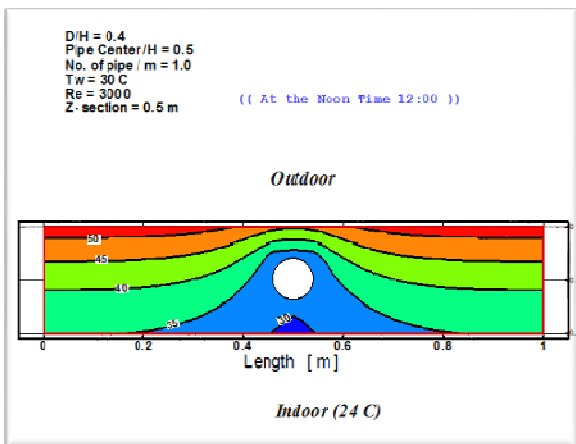


Fig. 7. Contour lines of temperature distribution when $D/H=0.4$, $T_w=30\text{ }^\circ\text{C}$, $Re=3000$.

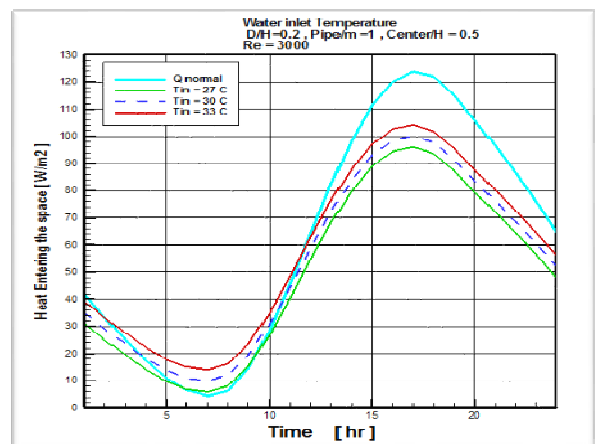


Fig. 10. Heat gain entering the space from the roof at different water inlet temperature versus time.

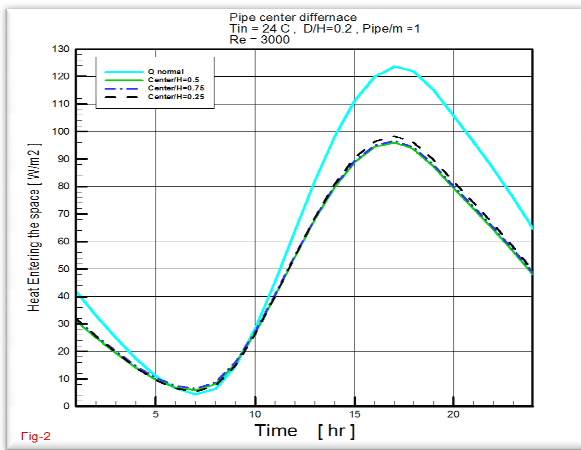


Fig. 11. Heat gain entering the space from the roof versus time at different pipe centers.

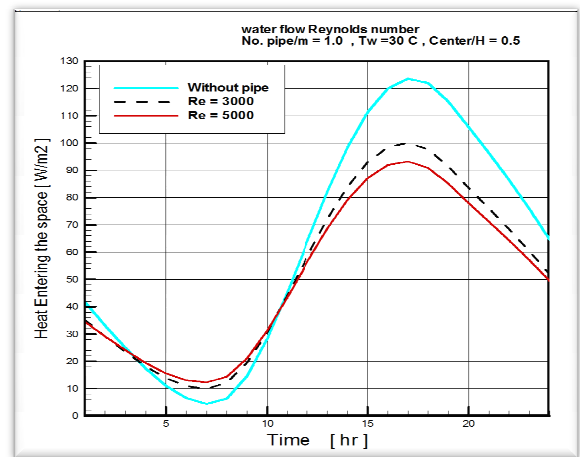


Fig. 14. Heat gain entering the space from the roof versus time at different Reynolds Numbers of inlet water.

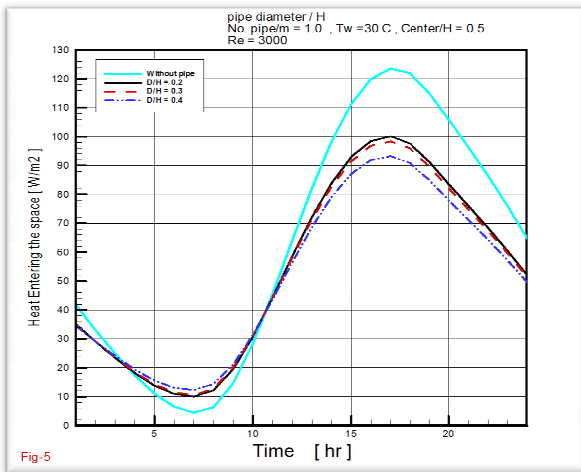


Fig. 12. Heat gain entering the space from the roof versus time at different D/H values.

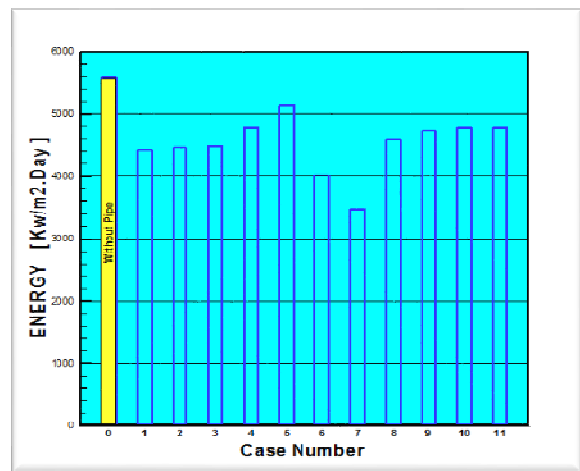


Fig. 15. Bar chart of energy entering the space from the roof per day for different cases.

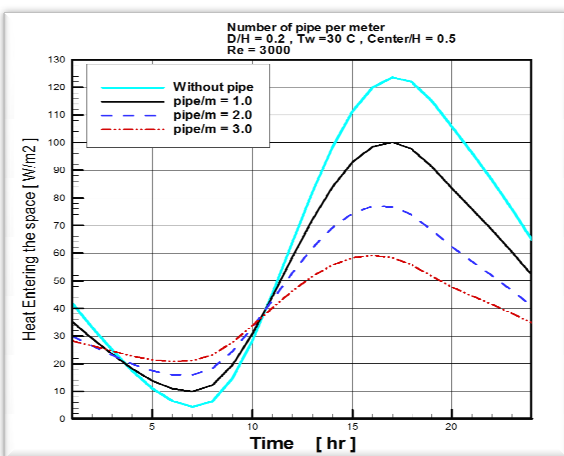


Fig. 13. Heat gain entering the space from the roof versus time at different Numbers of pipe.

Table 3
Cases parameter identifications.

Parameter	Case										
	1	2	3	4	5	6	7	8	9	10	11
Water inlet Temperature °C	27	27	27	30	33	30	30	30	30	30	30
D/H	0.2	0.2	0.2	0.2	0.2	0.2	0.2	0.1	0.3	0.1	0.1
No. PIPE/m	1	1	1	1	1	2	3	1	1	1	1
Pipe Centre/W	0.5	0.75	0.25	0.5	0.5	0.5	0.5	0.5	0.5	0.5	0.5
Reynolds number	3000	3000	3000	3000	3000	3000	3000	3000	3000	3000	5000

Nomenclature

c_p	specific heat (J/kg.°C)
D/H	pipe diameter to the wall Height ratio
D	pipe diameter (m)
h_f	convection heat transfer coefficient (W/m ² .°C)
h_f	convection heat transfer coefficient inside the pipe (W/m ² .°C)
k_f	fluid (water) thermal conductivity (W/m.°C)
Q_k	heat gain by water in k- element (W)
q_i	heat delivered to the node i by heat generation (W)
\dot{m}	water mass flow rate (kg/s)
Nu	Nusselt number : $Nu = \frac{hD}{k}$
Pr	Prandtl number: $Pr = \frac{c_p \mu}{k}$
R_{ij}	thermal conduction or convection resistance (m.°C/W)
Re	Reynolds number: $Re = \frac{\rho V D}{\mu}$
Rad	instantaneous solar radiation (W/m ²)
T_{pipe}	pipe surface temperature: (°C)
T_i^{p+1}	temperature on node i after a time increment $\Delta\tau$ (°C)
T_i^p	temperature on node i at particular time (°C)
T_{sat}	solar-air temperature (°C)
$T_{f_{k+1}}$	water element outlet temperature from the node k (°C)
T_{f_k}	water element inlet temperature in the node k (°C)
$T_{f_{ave}}$	water element average temperature (°C)
Two	outside wall temperature (°C)
Twi	inside wall temperature (°C)
T_{sat}	solar air temperature (°C)
$\Delta\tau$	time increment (s)
ΔV_i	volume of the element (m ³)
ρ	density (kg/m ³)
ϵ	surface emissivity

7. References

- [1] H. Heinrich and K. H. Dahlem, "Thermography of Low Energy Building", *Quantitative Infrared Thermography seminar*, QIRT, France, 2000.
- [2] Vechaphutti T., "A Study of Overall Thermal Transfer Values (OTTV) of High-rise Buildings as a Guideline for the Design of Energy Saving Building in Thailand", *Proceeding ICBEM'87* Lausanne, Switzerland, Sept. 28- Oct.2, 1987.
- [3] Sebastian Karlstrom, "Analysis of Thermally Active Ventilated Hollow Core Concrete Elements in a FEMLAB Environment Compared to measurements", *Division of Building Technology, Royal Institute of Technology, Brinellagen*, Volume (34), pages 100-14, Stockholm, Sweden, 2005
- [4] R. Saidur, M. Hasaunzaman, M. M. Hasan and H. H. Masjuki," Over all Thermal Transfer Value of Residential Building in Malaysia", *Journal of Applied Sciences*, 9(11), 2009.
- [5] T. Kiatsiriroat and M. Veekel, "Performance Analysis of cooled wall for Cooling Load Reduction in an Air-conditioned Room", *Asian Journal, Energy Environ.*, Vol. I, No. I, pp. 41-55, 2000.
- [6] Congnati, S.P., and Kindinis, A., "Thermal Mass Activation By Hollow Core Slab Copouied with Night Ventelation to Reduce Summer Cooling Load", *Building and Enviroment*, Volume (42), pages 3285-3297, 2007.
- [7] Sormunen Piia, Olof Granlund Oy, Helsinki, Laine Tuomas, and Saari Mikko," The Active Utilization of thermal mass of hollow core", *VTT Technical Research Centre of Finland*, Espoo, Finland, 2007.
- [8] Holman J. P, "Heat Transfer", fifth edition, McGraw-Hill publishing Company, 1981.
- [9] John H. Lienhard IV, "A Heat Transfer Textbook", third edition, 2004.

ترشيد في كسب الطاقة الحرارية بأستخدام الأنابيب المدفونة في السقف

أحمد عبد محمد صالح

قسم الهندسة الميكانيكية / الجامعة التكنولوجية
البريد الإلكتروني: aamsaleh60@yahoo.com

الخلاصة

في هذا العمل أجريت دراسة عديدة لمعرفة تأثير أنابيب الماء المدفونة في السقوف على تقليل الكسب الحراري ومنع انتقال الحرارة الى داخل الفضاءات المكيفة. وأظهرت نتائج البحث أن هنالك إمكانية لتقليل الكسب الحراري عند قيم محددة من العوامل المؤثرة مثل عدد الأنابيب للمتر الواحد من عرض السقف ونسبة قطر الأنبوب الى سمك السقف (D/W) و درجة حرارة الماء الداخل الى الأنبوب. حيث بينت النتائج ان هنالك تخفيض بنسبة ٤٠ % مقارنة مع السقف الخالي من الأنابيب عندما يكون عدد الأنابيب للمتر الواحد هو ٣ ونسبة قطر الأنبوب الى سمكه بحدود ٠.٥ ودرجة حرارة الماء الداخل الى الأنبوب هي $30^{\circ}C$ ، بينما بلغت أقل نسبة من التخفيض وهي ١٤ % عند عدد الأنابيب يساوي ١ لكل متر من عرض السقف ونسبة قطر الأنبوب الى سمك السقف هي ٠.٥ ايضاً ولكن درجة حرارة الماء الداخل الى الأنابيب هي $33^{\circ}C$ وكلاهما عند عدد رنولدز للماء المناسب خلال الأنبوب هو ٣٠٠٠ . كما وأظهرت النتائج بأن هنالك تأثير بسيط جداً على كمية الحرارة المنتقلة خلال السقف عند تغيير موقع مركز الأنبوب داخل السقف.